

## Research Article

# Biosynthesis of titanium dioxide nanoparticles using *Hypericum perforatum* and *Origanum vulgare* extracts and their main components, hypericin and carvacrol as promising antibacterial agents

Mojtaba Khaksarian, Mahmoud Bahmani, Morovat Taherikalani, Behnam Ashrafi, Mahmoud Rafieian-Kopaei, Naser Abbasi

**Mojtaba Khaksarian**, Department of Physiology and Pharmacology, School of Medicine, Razi Herbal Medicines Research Center, Lorestan University of Medical Sciences, Khorramabad, Iran

**Mahmoud Bahmani**, Biotechnology and Medicinal Plants Research Center, Ilam University of Medical Sciences, Ilam, Iran; Razi Herbal Medicines Research Center, Lorestan University of Medical Sciences, Khorramabad, Iran

**Morovat Taherikalani**, Department of Microbiology, School of Medicine, Lorestan University of Medical Sciences, Khorramabad, Iran

**Behnam Ashrafi**, Razi Herbal Medicines Research Center, Lorestan University of Medical Sciences, Khorramabad, Iran

**Mahmoud Rafieian-Kopaei**, Medical Plants Research Center, Basic Health Sciences Institute, Shahrekord University of Medical Sciences, Shahrekord, Iran

**Naser Abbasi**, Biotechnology and Medicinal Plants Research Center, Ilam University of Medical Sciences, Ilam, Iran; department of Pharmacology, Faculty of Medicine; Ilam University of Medical Sciences, Ilam, Iran

**Correspondence to: Dr. Mahmoud Bahmani**; Biotechnology and Medicinal Plants Research Center, Ilam University of Medical Sciences, Ilam, Iran. Bangjib Campus, Postal Code: 6939177143; [mahmood.bahmani@gmail.com](mailto:mahmood.bahmani@gmail.com)

DOI: 10.19852/j.cnki.jtcm.2022.02.002

Received: October 28, 2020

Accepted: March 3, 2021

Available online: April 1, 2022

## Abstract

**OBJECTIVE:** To evaluate the anti-bacterial activities of titanium dioxide (TiO<sub>2</sub>) nanoparticles of *Origanum* (O.) *vulgare* and *Hypericum* (H.) *perforatum* extracts, carvacrol and hypericin against *Staphylococcus* (S.) *aureus*.

**METHODS:** In this study, TiO<sub>2</sub> nanoparticles of O. *vulgare* and H. *perforatum* extracts, carvacrol and hypericin, were prepared and their antibacterial effects were evaluated against *Staphylococcus* (S.) *aureus*. In this study, scanning electron microscope, fourier transform infrared spectrometer, atomic force microscopy, dynamic light scattering and zeta potential were used to investigate the structure of synthesized drugs.

**RESULTS:** Anti-bacterial activity of synthesized NPs was tested by minimum inhibitory concentration (MIC),

minimum bactericidal concentration and disc diffusion method. MICs of TiO<sub>2</sub>-NPs synthesized using O. *vulgare*, H. *perforatum*, carvacrol and hypericin and TiO<sub>2</sub> were obtained 250, 62.5, 250, and 250, and 500 µg/mL, respectively. The MBCs for all of these were obtained 1000 µg/mL.

**CONCLUSION:** Green-synthesized of TiO<sub>2</sub> nanoparticles provides a promising approach to the use of O. *vulgare* and H. *perforatum*, carvacrol and hypericin as novel agents and safer antibacterial compounds, especially anti-S. *aureus* compounds.

© 2022 JTCM. All rights reserved.

**Keywords:** plant, medicinal; medicine, traditional; anti-infective agents; active ingredient; nano-compounds

## 1. INTRODUCTION

*Staphylococcus* (S.) species are one of the most common causes of nosocomial infections in the world.<sup>1,2</sup> Among S. species, S. *aureus* has the highest pathogenicity.<sup>3</sup> S. *aureus* is one of the most important causes of community-acquired infections, which can be a major contributor to hospital infections such as bacteremia, endocarditis, skin infections, osteomyelitis, and toxic shock syndrome.<sup>4</sup> S. *aureus* is a gram-positive and catalase-positive bacterium and has spherical form, which usually makes irregular clusters similar to grapes. *Staphylococci* infections in recent years have been increasing due to the spread of resistant strains, increase in patients with immune deficiency, and excessive use of medical devices such as catheters. S. *aureus* is usually resistant to antibiotics such as penicillin and vancomycin.<sup>5,6</sup> Today, antibiotic resistance in resistant bacteria, especially *Staphylococci*, is of great importance to physicians. Hence, preparation of new drugs to combat bacterial resistance is crucial. Nowadays, nanodrugs are used in natural compounds and pharmaceutical industries in order to reduce the use of chemical drugs.<sup>7</sup> Titanium dioxide (TiO<sub>2</sub>) is a metal that has many applications in the nanotechnology industry due to its

photocatalytic properties.<sup>8</sup> TiO<sub>2</sub> has several phases, crystalline, anatase, rutile and brookite, out of which anatase and rutile phases are more important due to photocatalytic properties.<sup>9</sup> It has low toxicity, chemical stability and low cost.<sup>10</sup> TiO<sub>2</sub> also has small size, high reactivity, chemical composition, high surface area per unit of mass.<sup>11</sup> For these reasons, it currently has many applications in the pharmaceutical, medical, and cosmetic industries.<sup>12</sup> The efficiency of TiO<sub>2</sub> is strongly influenced by the size, shape, and crystalline structure of nanoparticles.<sup>13</sup> It has antimicrobial and antibacterial properties and has no toxic effects.<sup>14-17</sup> Traditionally, because of the low solubility and low toxicity of synthesized TiO<sub>2</sub> NPs, it has been used as negative control in studies.<sup>18</sup> Among the different approaches to biosynthesis or green synthesis of materials, use of medicinal plants and herbal extracts is very common these days.<sup>19</sup> Green synthesis of herbal extracts is a safe way to reduce the risks of chemical drugs.<sup>20</sup> Medicinal plants and plant extracts, and certain microorganisms such as fungi and bacteria and probiotics are used as biological mediators for the synthesis and biological targets.<sup>21-23</sup> In this study, the plants *Hypericum perforatum* (*H. perforatum*) and *Origanum vulgare* (*O. vulgare*) and their active ingredients, i.e. carvacrol and hypericin were synthesized using TiO<sub>2</sub> and their antibacterial effects were investigated against *S. aureus*.

## 2. MATERIALS AND METHODS

### 2.1. Medicinal plants

In this study, *H. perforatum* (Herbarium code 48120) and *O. vulgare* (Herbarium code 48119) plants were collected from of Mazandaran province in northern Iran. The plants are collected and used for testing. The main active ingredients of the plants (carvacrol and hypericin) were purchased from Sigma-Aldrich and they used for the study.

### 2.2. Preparation of hydroalcoholic extract

The hydroalcoholic extract of the plant was prepared according to Bahmani *et al.*<sup>21</sup>

### 2.3. Synthesis of TiO<sub>2</sub> NPs

For synthesis of herbs and compounds was carried out with modified method of Sanker *et al.*<sup>24</sup> (2013). 1000 mg of hydroalcoholic of plant extracts and 30 mg of carvacrol or hypericin were added to 90 mL of TiO<sub>2</sub> in an Erlenmeyer flask with shaker. Each 30 min of shaking the solution, it was increased to 5 min at 50 °C to synthesize the materials and compounds. After 5 h of continuous stirring, the solution obtained in 50 mL falcons was centrifuged at 12 000 rpm at 4 °C for 15 min.

### 2.4. Characterization of synthesized NPs

Different techniques were used to determine the size, shape, and stability of synthesized NPs included

scanning electron microscope (SEM), dynamic light scattering (DLS), Fourier-transform infrared spectroscopy (FTIR) and zeta potential, as well as atomic force microscope (AFM).

### 2.5. *In vitro* antibacterial activity of synthesized NPs

The evaluation of antibacterial effect of synthesized NPs was carried out using minimum inhibitory concentration (MIC), minimum bactericidal concentration (MBC) and disc diffusion method.

MIC and MBC were determined using the broth microdilution method proposed by the clinical and Laboratory Standards Institute (CLSI).<sup>25</sup> First, a stock solution was prepared from TiO<sub>2</sub> NPs synthesized using *H. perforatum* (5.000 ppm), *O. vulgare* (5.000 ppm), carvacrol (1.000 ppm), and hypericin (1.000 ppm). Then, 50 µL of sterile Mueller-Hinton broth was added to all wells. Next, 50 µL of stock solutions of NPs were added to the first and second rows and dilution were performed on the second to the tenth rows. Finally, 50 µL of the 24 h *S. aureus* (ATCC 12600) culture, equivalent to 0.5 McFarland turbidity ( $5 \times 10^5$  CFU/mL), was added to each of the second to the tenth wells, and the plates were incubated at 37 °C for 24 h. Methicillin (Sigma-Aldrich) was used as a positive control. After 24 h of incubation, 30 µL of 2,3,5-triphenyltetrazolium chloride was added to the visual index for bacterial growth.<sup>25</sup> Colorless wells were considered to indicate MIC.<sup>25</sup> The proposed CLSI protocol (2009) was also used to determine the MBC. Briefly, 5 µL of the solution of the wells (following the wells in which MIC formed) was inoculated on the plates containing Mueller-Hinton broth and placed at 37 °C for 24 h. The concentration at which no colony formed on the plate was considered to be MBC.<sup>25</sup>

To investigate the inhibition zone, on the Mueller-Hinton agar, bacterial culture of a suspension with 0.5 McFarland turbidity was inoculated into the medium with sterile swab and a disc of antibiotic methicillin was left on the medium. In addition, 40 µL of standard stocks of TiO<sub>2</sub> NPs synthesized with *H. perforatum*, *O. vulgare*, carvacrol and hypericin were added to the blank discs and left on the medium. The plates were then incubated at 37 °C for 24 h. The test was repeated three times and the results were expressed as mean ± standard deviation. The growth inhibition zone was measured by the culis.<sup>25</sup> The plates were then incubated at 37 °C for 24 h. The growth inhibition zone was measured by caliper. Each drug group was repeated three times.

### 2.6. Statistics analysis

Regarding the microbial tests such as MIC, MBC and disc diffusion method were repeated three times, the mean ± standard deviation was used for data analysis and reporting. In this study, mean ± standard deviation was used through Microsoft Office Pro Plus 2016 software (Excel).

### 3. RESULTS

The color of pure TiO<sub>2</sub> remains unchanged without the use of plant extracts, but when TiO<sub>2</sub> reacts with the plant extract or compound, color change occurs. After the reaction of titanium isopropoxide separately with *H. perforatum*, *O. vulgare*, hypericin, and carvacrol, their colors were changed. After the reaction of TiO<sub>2</sub> with *H. perforatum*, the color of extract was changed from dark green to light green. The reaction of TiO<sub>2</sub> with *O. vulgare*, the color changed from dark red to bright red. The reaction of TiO<sub>2</sub> with hypericin caused the color to change from red to pale hepatic. Also, the TiO<sub>2</sub> reaction with carvacrol changed the color from white to milky.

The FTIR spectra of synthesized TiO<sub>2</sub> NPs using different extracts and compounds were shown in Figure 1. Comparison of FT-IR spectra of synthesized TiO<sub>2</sub> NPs using *O. vulgare* and carvacrol shows high similarities. Also, this situation was observed for FT-IR spectra of synthesized TiO<sub>2</sub> NPs using *H. perforatum* and hypericin. The reasons for this phenomenon can be attributed to active compounds of these extracts. As we know, the active compounds of *O. vulgare* and *H. perforatum* are carvacrol and hypericin, respectively.

The morphology and size of nanoparticles were also investigated with SEM. The synthesized TiO<sub>2</sub> NPs using *H. perforatum* show spherical morphology with a diameter of 37.6-81.8 nm (Figure 2A). TiO<sub>2</sub> NPs synthesized using hypericin (Figure 2B). The synthesized TiO<sub>2</sub> NPs with *O. vulgare* extract represents spherical morphology for TiO<sub>2</sub> NPs with a diameter of 42.1-107 nm (Figure 2C). The morphology observed by the SEM images for the TiO<sub>2</sub> NPs synthesized using carvacrol (Figure 2D) and are also spherical and have diameters with the ranges of 29-52.2 nm and 42.1-60.1, respectively.

In the below, 2 μm × 2 μm images obtained by the Atomic Force Microscopy Analysis (AFM-Nano Surf, Switzerland) are provided below. The images of all samples were prepared by casting a solution of the samples on silicon (111) to create a thin layer of them. The mean roughness obtained for TiO<sub>2</sub> NPs synthesized using *O. vulgare*, *H. perforatum*, carvacrol and hypericin were equal to 52.33, 39.81, 55.39 and 90.26 nm, respectively. In samples of TiO<sub>2</sub> NPs synthesized using *H. perforatum* and NPs synthesized using hypericin, the

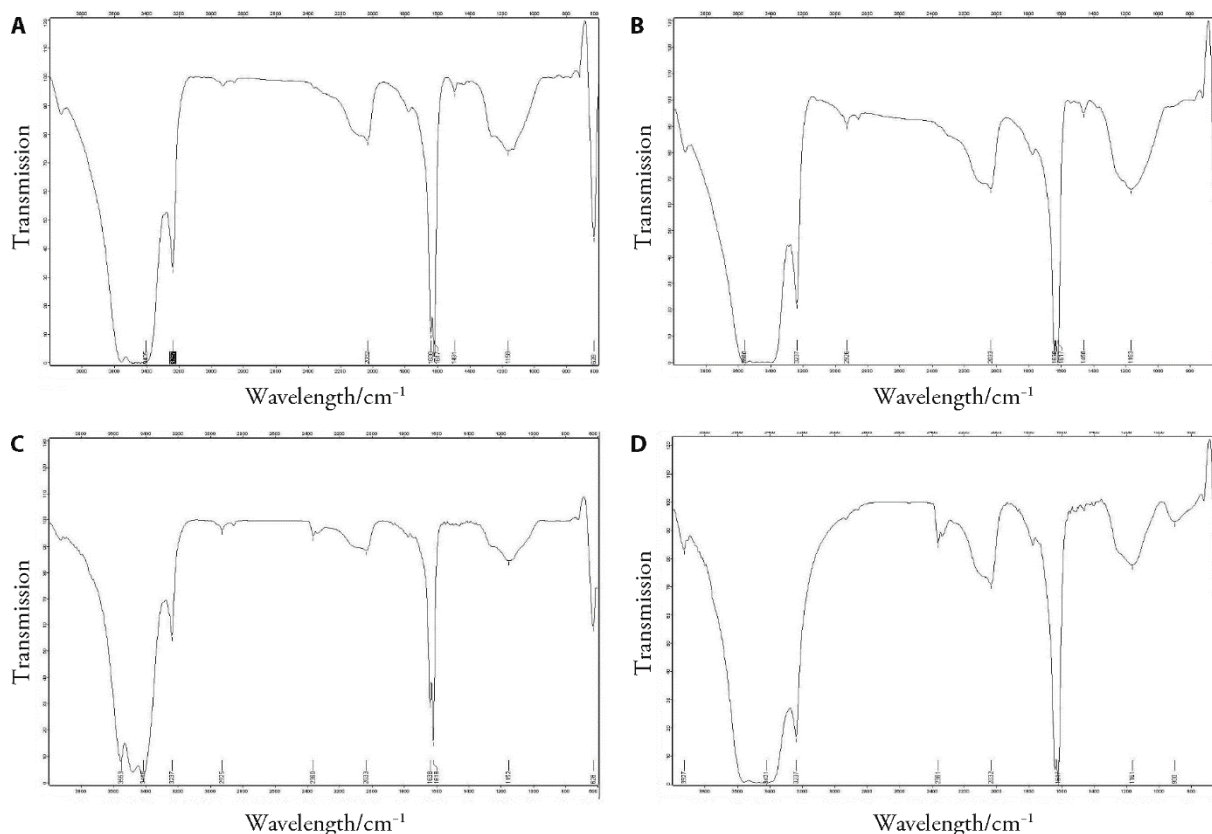


Figure 1 FTIR spectra of synthesized titanium dioxide nanoparticles

A: hydroalcoholic extract *Hypericum perforatum*; B: hypericin; C: hydroalcoholic extract of *Origanum vulgare*; D: carvacrol. FTIR: Fourier transform infrared spectrometer. Based on the analysis of the spectra of hydroalcoholic extracts of synthesized using *Origanum vulgare* is observed in wavelengths of 1225 cm<sup>-1</sup> (C-O stretch) and 625 cm<sup>-1</sup> (C-Br stretch) of titanium bond. It is also observed for *Origanum vulgare* NPs. at a wavelength of 3352 O-H stretch. TiO<sub>2</sub> NPs. using carvacrol is observed in titanium at wavelengths of 1161 cm<sup>-1</sup> (C-O stretch) and 627 cm<sup>-1</sup> (C-Br stretch). It is also observed for TiO<sub>2</sub> NPs. synthesized using carvacrol at a wavelength of 3927 cm<sup>-1</sup> (O-H stretch). TiO<sub>2</sub> NPs. synthesized using hydroalcoholic extract of *Hypericum perforatum* is also observed at a wavelength 1158 cm<sup>-1</sup> (C-O stretch) and 628 cm<sup>-1</sup> (C-Br stretch) are observed bond with titanium. TiO<sub>2</sub> NPs. synthesized using hypericin with wavelengths 1154 cm<sup>-1</sup> (C-O stretch) and 626 cm<sup>-1</sup> (C-Br stretch) are observed bonds with titanium.

layer growth of the samples is clearly visible on the surface, but in the sample of TiO<sub>2</sub> NPs synthesized using *H. perforatum*, island growth also occurred, while in the sample of TiO<sub>2</sub> NPs synthesized using hypericin, the surface is rougher, but the growth all over the surface is more uniform. In the sample of the TiO<sub>2</sub> NPs synthesized using *O. vulgare*, island growth occurred in some spots and there was a large distance between the peaks and the valleys created on surface, which made the surface of this sample less uniform than those of the other samples, while in the TiO<sub>2</sub> NPs synthesized using carvacrol, in all over the surface, the particles' growth was also uniform. Based on the results, the synthesis of all the nanodrugs was done well and the particle size was standard and corresponded to the particles observed in the AFM microscope (Figure 3).

The measurements of the particle size by DLS showed that TiO<sub>2</sub> NPs using *H. perforatum* (Figure 4A) 951.4 and 0.640, TiO<sub>2</sub> NPs using hypericin (Figure 4B) 5949 and 0.960 (Figure 4C). Z-average and pdi were respectively obtained for TiO<sub>2</sub> NPs 1, and for TiO<sub>2</sub> NPs using carvacrol (Figure 4D) 2931 and 0.640. The results showed that the particle size was well measured by the DLS.

Accordingly, synthesized TiO<sub>2</sub> NPs using *H. perforatum* extract had a potential zeta equal to +25.4 mV (Figure 5A). In addition, the zeta potential of TiO<sub>2</sub> NPs synthesized using hypericin, *O. vulgare* and carvacrol are equal to *O. vulgare*, carvacrol, and hypericin are equal to

+5.46 mV (Figure 5B), -29.1 mV (Figure 5C) and +22.2 mV (Figure 5D), respectively. Zeta potential results show that synthesized TiO<sub>2</sub> NPs using *H. perforatum*, *O. vulgare* and carvacrol are stable whereas the synthesized TiO<sub>2</sub> NPs using hypericin has not favorable stability.

MIC of TiO<sub>2</sub> NPs synthesized using *O. vulgare*, *H. perforatum*, carvacrol and hypericin and TiO<sub>2</sub> NPs was obtained 250, 62.5, 250, and 250, and 500 µg/mL, respectively. MBC for these was obtained 1000 µg/mL. MIC, MBC and zone inhibition diameter of the groups were shown in Table 1.

#### 4. DISCUSSION

Based on the results, it was found that the highest MIC was obtained for the TiO<sub>2</sub> NPs synthesized using *H. perforatum*, followed by the TiO<sub>2</sub> NPs synthesized using *O. vulgare*, carvacrol, and hypericin. The lowest inhibitory effect was obtained for pure TiO<sub>2</sub> NPs. In other words, although TiO<sub>2</sub> NPs alone exert antibacterial effect on *S. aureus*, all of the herbal NPs and their compounds have lower MICs and greater antibacterial effects than TiO<sub>2</sub> NPs.

The results of the study of Nostro *et al*<sup>26</sup> on the anti-*S. aureus* effects of *Origanum majorana* essential oil and carvacrol, showed that the MIC of *O. vulgare* essential oil and carvacrol were 0.062% and 0.015% v/v and their MBCs 0.125% and 0.062% v/v, respectively. The results of this study showed that the tea of pure *H. perforatum* on resistant and susceptible strains of *S. aureus* had growth inhibition zone diameters of 13 and 12.4 mm,

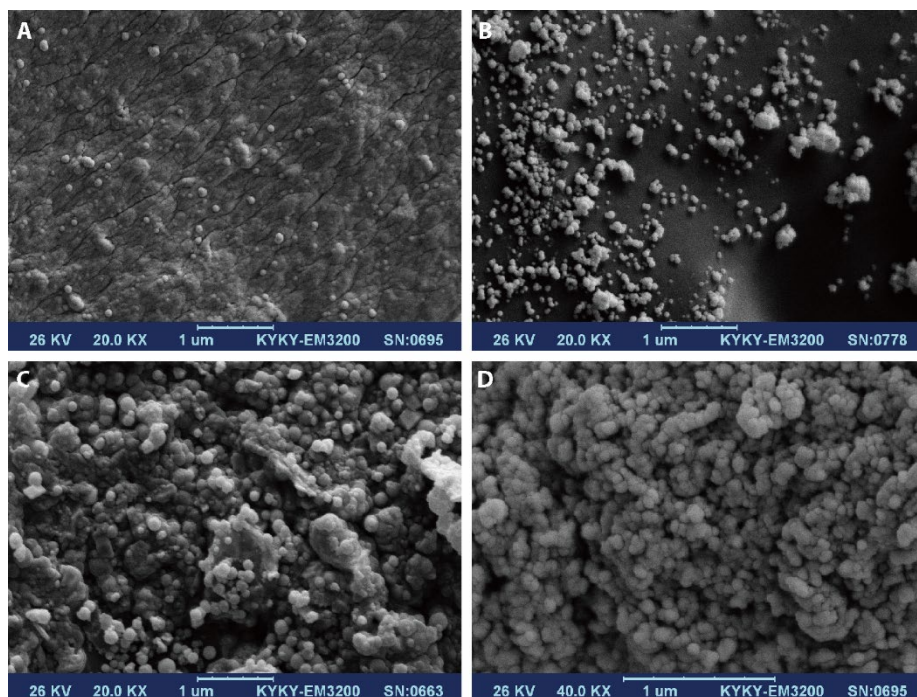


Figure 2 Scanning electron microscope images of synthesized titanium dioxide nanoparticles

A: *Hypericum perforatum*; B: hypericin; C: *Origanum vulgare*; D: carvacrol. The properties of NPs synthesized using atomic force microscope are presented in a three-dimensional visualization. The morphology of a rugged surface with the presence of both individual nanoparticles and agglomerates are described. Strong crystalline nature can be seen in diagonal figures containing mountains.

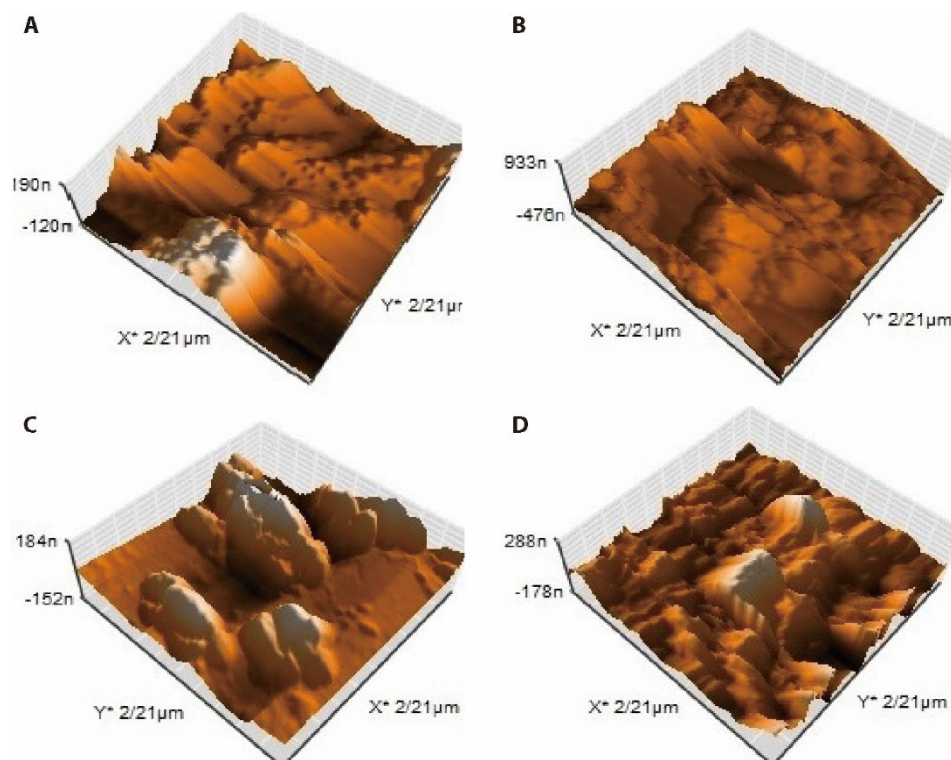


Figure 3 Atomic force microscopy images of synthesized titanium dioxide nanoparticles  
A: Hypericum perforatum; B: hypericin; C: Origanum vulgare; D: carvacrol.

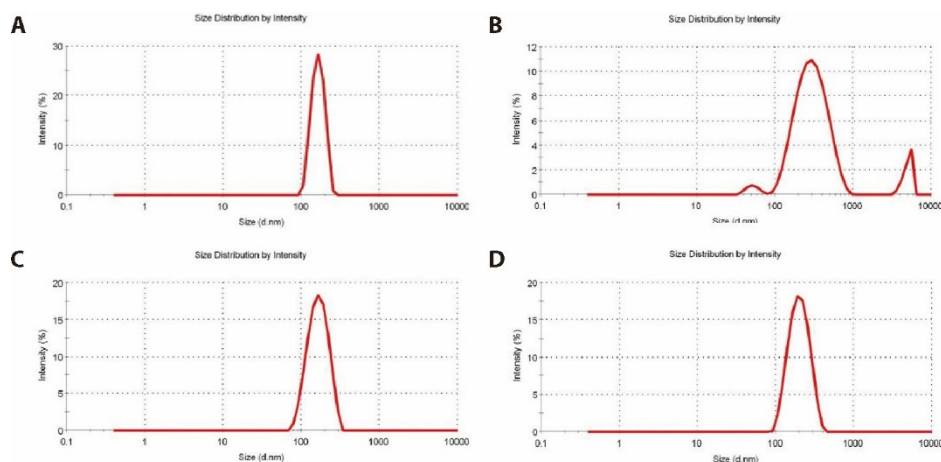


Figure 4 Dynamic light scattering analysis of titanium dioxide nanoparticles synthesized  
A: Hypericum perforatum; B: hypericin; C: Origanum vulgare; D: carvacrol.

respectively.<sup>27</sup> The study of García *et al*<sup>28</sup> showed that hypericin was able to deactivate and produce antimicrobial effect on the biofilms of the methicillin resistant strains of *S. aureus*. In another study, hypericin-photodynamic activation in combination with acetyl-cysteine was found to have a significant potential for eradicating mature biofilms from *S. aureus*.<sup>29</sup> The results of the studies indicated the anti-*S. aureus* effects of the total essential oil, extract, and active ingredients, and the result of our study demonstrated the anti-staphylococcal effects of the NPs of these plants.

Our results are consistent with the cited studies. Photodynamic activity is one of the factors influencing the antimicrobial activity of plant compounds. Studies have shown that TiO<sub>2</sub> NPs are trapped on the surface of

the bacteria, and thus the absorption of TiO<sub>2</sub> NPs on the surface.

In this study, the pharmaceutical agents synthesized using TiO<sub>2</sub> were found to produce antibacterial effects due to the presence of TiO<sub>2</sub> and its NPs through photocatalytic oxidation. Studies have shown that due to exposure to ultraviolet radiation or sunlight, TiO<sub>2</sub> has antimicrobial effects because of its strong oxidation properties. The microbe surface is the primary target of the oxidative attack, and TiO<sub>2</sub> particles cause contact with the microbe and produce antimicrobial effects by absorbing the radiation.<sup>30</sup> Since each material has its own atomic bonds, there are no two compounds with an exactly identical infrared spectrum. Therefore, infrared spectroscopy can be an efficient method to better identify

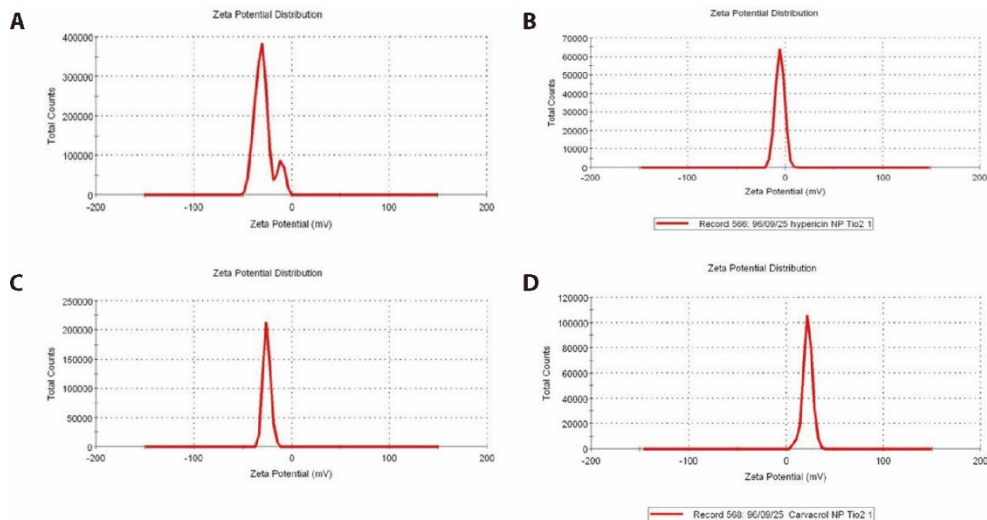


Figure 5 Zeta potential measurements of synthesized titanium dioxide nanoparticles  
A: *Hypericum perforatum*; B: hypericin; C: *Origanum vulgare*; D: carvacrol.

Table 1 Minimum inhibitory concentration, minimum bactericidal concentration and zone inhibition diameter of the groups

Group	Minimum inhibitory concentration ( $\mu\text{g/mL}$ )	Minimum bactericidal concentration ( $\mu\text{g/mL}$ )	Mean $\pm$ Standard deviation (mm)
Titanium dioxide nanoparticles synthesized using <i>Origanum vulgare</i>	250	1000>	8.00 $\pm$ 0.70
Titanium dioxide nanoparticles synthesized using Hypericum perforatum	62.5	1000>	7.33 $\pm$ 0.40
Titanium dioxide nanoparticles synthesized using carvacrol	250	1000>	8.00 $\pm$ 0.00
Titanium dioxide nanoparticles synthesized using hypericin	250	1000>	34.33 $\pm$ 0.40
Titanium dioxide nanoparticles	500	1000>	10.00 $\pm$ 0.00
Methicillin	384	384	22.00 $\pm$ 0.81

different types of materials, types of functional groups, and the bonds in their molecules. Therefore, similar peaks represent the presence of the same materials. Based on the results, the absorption peaks observed in the FTIR graphs obtained from  $\text{TiO}_2$  NPs synthesized using *H. perforatum* indicated the bonds O-H, N-H, C-H, O=C=O, C=C, N-O, and S=O, which indicates the existence of the same groups in the hydroalcoholic extract of *H. perforatum*, which is identical to the  $\text{TiO}_2$  NPs synthesized using hydroalcoholic *H. perforatum* extract. This determines that the mentioned functional groups play a role in the synthesis of NPs. In addition, the absorption peaks observed in the FTIR graph obtained from  $\text{TiO}_2$  NPs synthesized using hypericin and other groups indicate the role of the above-mentioned functional groups in the synthesis of NPs. Functional groups reduce the bioreduction of  $\text{TiO}_2$  particles into  $\text{TiO}_2$  NPs. The results of the study by Huck-Pezzei *et al.*<sup>31</sup> showed that in the FTIR test, *H. perforatum* had constituents at 865-3300 nm wavelengths and contained carbohydrate, nucleic acid, ether, phospholipid, lignin, etc. The results of the study by Galehassadi *et al.*,<sup>32</sup> on the FTIR of *O. vulgare*, revealed that the plant had an OH phenol band at a wavelength of  $3392\text{ cm}^{-1}$ . It also had C-H stretching bands, asymmetric stretching vibrations of aliphatic C-H, symmetric stretching vibrations of aliphatic C-H, and aromatic C=C stretching at wavelengths of 3020, 2927, 2869, and  $1620/\text{cm}$ ,

respectively. Hydroalcoholic extracts of *O. vulgare* and *H. perforatum* have bioactive substances that play an important role in the synthesis of  $\text{TiO}_2$  NPs. Based on the results obtained in this study, all the herbal NPs and their active ingredients had good antibacterial effect on  $\text{TiO}_2$  NPs.

Metal oxide NPs exhibited different antibacterial properties depending on the surface area to volume ratio. The results of the studies show that gram-positive pathogenic bacteria exhibit greater resistance against metal NPs than Gram-negative pathogenic bacteria, which can be related to the structure of the cell wall.<sup>33</sup> It seems that the released  $\text{TiO}_2$  ions in the culture medium that have positive electrical charge and cause the binding to bacterial surface proteins are the main causes of bacteriostatic and bactericidal properties of the NPs synthesized in this study. In general, the charge of the bacteria is negative and the charge of the nanoparticle positive. The same difference between the negative charge of the microorganisms and the positive charge of the nanoparticle acts as an absorbing electromagnetic load between the microbe and the nanoparticle, and causes the nanoparticle to bind to the cell surface, and thus can lead to cell death.<sup>34</sup> In another mechanism of action, the ions released from the NPs are responsible for reaction and binding to the thiol groups of the surface proteins of bacterial cells.<sup>35</sup> Besides that, NPs delay the bacterial cell adhesion and biofilm formation, which

makes some groups of bacteria unable to stabilize and proliferate.<sup>36</sup> In addition, NPs themselves can penetrate into bacteria and cause leakage of intracellular materials out of microorganisms.<sup>37</sup> The ability of TiO<sub>2</sub> NPs to produce reactive oxygen species, and their toxicity and application<sup>38</sup> has attracted significant attention. Antibacterial activity of TiO<sub>2</sub> leads to the production of reactive oxygen species, particularly hydroxyl and peroxide free radicals under ultraviolet radiation through oxidizing and reducing pathways.<sup>39</sup> The causes of increased antibacterial effect of green synthesis in this study include the synergistic effects of TiO<sub>2</sub> NPs and *O. vulgare* and *H. perforatum*, carvacrol, and hypericin, which have antibacterial activity and produce greater antimicrobial effect by increasing the resulting surface and structure.

The study of Sankar *et al*<sup>24</sup> on the synthesis of aquatic *O. vulgare* extract synthesized using TiO<sub>2</sub> NPs, showed the size of the NPs was 341 nm and the negative potential 27.3 mV. In our study, hydroalcoholic *O. vulgare* extract, based on SEM, had a size of 42.1-107 nm, and based on the AFM test, a mean roughness of 52.33 nm and negative potential of -25.4. Our study showed that hydroalcoholic extract had a higher capacity for green TiO<sub>2</sub> synthesis and led to smaller NPs than the aqueous extract. Negative charge provides greater stability for TiO<sub>2</sub> and prevents accumulation and increase in the density of NPs.<sup>40</sup> In our study, TiO<sub>2</sub> NPs synthesized using *O. vulgare* (-25.4 mV), *H. perforatum* (-29.1 mV), and carvacrol (22.1 mV), had high stability while the TiO<sub>2</sub> NPs synthesized using hypericin with -5.46 mV potential had a synthetically low stability. The antibacterial effect of the NPs produced against the gram-positive *S. aureus* showed that the MICs of the TiO<sub>2</sub> NPs synthesized using *H. perforatum* and *O. vulgare*, hypericin, and carvacrol were 62.5, 250, 250 and 250 µg/mL, respectively. The MBC of the produced NPs against *S. aureus* showed that the MBC of the TiO<sub>2</sub> NPs synthesized using *H. perforatum* and *O. vulgare*, hypericin, and carvacrol was all equal to 1000 µg/mL. The diameter of the growth inhibition zone of the TiO<sub>2</sub> NPs synthesized using *H. perforatum* and *O. vulgare*, hypericin, and carvacrol was obtained 7.3 ± 0.4, 8.0 ± 0.7, 8.0 ± 0.0, and 34.3 ± 0.4. Water-soluble heterocyclic compounds, such as flavones and ligands, reduce and absorb NPs. Functional groups associated with this cause bioreduction of TiO (OH)<sub>2</sub> into TiO<sub>2</sub> NPs.<sup>41</sup> Flavones and ligands in *O. vulgare* and *H. perforatum* are probably bioreductive agents of synthesized TiO<sub>2</sub> NPs, which result in a more effective antibacterial effect of green synthesis. The results of the study by Barzegar *et al*<sup>42</sup> showed that 1.5% TiO<sub>2</sub> NPs caused cell death of *S. aureus* after 24 h. Its mechanism of action is through the peroxidation of the cyclic phospholipid membrane and disruption of membrane permeability. The results of the study of Saadatmand *et al*<sup>43</sup> showed that chitosan-TiO<sub>2</sub> nanocomposite was nearly 100% effective on the growth of *S. aureus*. The results of a study showed that TiO<sub>2</sub> NPs in combination

with β-lactam, cephalosporins, aminoglycosides, glycopeptides, macrolides, lincosamides, and tetracycline were able to exhibit antimicrobial activity against methicillin-resistant *S. aureus*.<sup>44</sup> Antimicrobial properties of medicinal plants are usually due to phenolic compounds, saponins, and flavonoids in their structure. These commonly used ingredients usually affect the permeability of the cytoplasmic membrane and its structural enzymes and exert their medicinal effect. Therapeutic and medicinal effects of herbal and aromatic plants through their active ingredients and antioxidants.<sup>45,46</sup> It is essential to find nanodrugs that are synthesized from medicinal plants and used as medicine.<sup>47-54</sup> Effective compounds and herbal antioxidants can be used as effective drugs for medicinal purposes.<sup>55-62</sup> Based on the results of this study, we can conclude that TiO<sub>2</sub> NPs (synthesized using *O. vulgare*, *H. perforatum*, carvacrol, and hypericin) alone have anti-*S. aureus* properties. The physicochemical properties of their NPs were confirmed by the use of the DLS, SEM, FTIR, AFM, and Zeta potential. All four synthesized TiO<sub>2</sub> NPs had optimal antimicrobial effects against *S. aureus*. The results provide conclusive evidence for the antibiotic activity of synthesized TiO<sub>2</sub> NPs. The authors are confident that in the near future, green-synthesized TiO<sub>2</sub> NPs can be used as a new and effective antibiotic and therapeutic agent for the treatment of infectious diseases. Green synthesized provide a promising approach to the use of extracts of *O. vulgare* and *H. perforatum*, and carvacrol and hypericin to fulfill the industrial need for antimicrobial compounds, especially anti-*S. aureus* agents, that are also new, simplified, low cost, environmentally friendly, and recyclable.

## 5. ACKNOWLEDGMENT

This article was extracted from PhD thesis of Dr. Mahmoud Bahmani M with code A-10-1379-1. The authors would like to express their gratitude for financial support of the Research and Technology Deputy of Lorestan University of Medical Sciences, Khorramabad, Iran.

## 6. REFERENCES

1. Kilic A, Basustaoglu AC. Double triplex real-time PCR assay for simultaneous detection of *Staphylococcus aureus*, *Staphylococcus epidermidis*, *Staphylococcus hominis*, and *Staphylococcus haemolyticus* and determination of their methicillin resistance directly from positive blood culture bottles. *Res Microbiol* 2011; 162: 1060-6.
2. Jadhav S, Hussain A, Devi S, et al. Virulence characteristics and genetic affinities of multiple drug resistant uropathogenic *Escherichia coli* from a semi urban locality in India. *PLoS One* 2011; 6: 18063.
3. El Farran CA, Sekar A, Balakrishnan A, Shanmugam S, Arumugam P, Gopalswamy J. Prevalence of biofilm-producing *Staphylococcus epidermidis* in the healthy skin of individuals in Tamil Nadu, India. *Indian J Med Microbiol* 2013; 31: 19-23.
4. Weichhart T, Horky M. Functional selection of vaccine candidate peptides from *Staphylococcus aureus* whole-genome expression libraries *in vitro*. *Infect Immunity* 2003; 71: 4633-41.
5. Li W. Antibacterial activity and mechanism of silver

- nanoparticles on *Escherichia coli*. *Appl Microbiol Biotechnol* 2010; 2: 23-7.
6. Tenover FC. Mechanisms of antimicrobial resistance in bacteria. *Am J Infect Control* 2006; 34: 3-10.
  7. Santhoshkumar T, Abdul Rahuman A, Jayaseelan CH, et al. Green synthesis of titanium dioxide nanoparticles using *Psidium guajava* extract and its antibacterial and antioxidant properties. *Asian Pac J Trop Med* 2014; 968-76.
  8. Sawhney APS, Condon B. Modern applications of nanotechnology in textiles. *Textile Research J* 2008; 78: 731-9.
  9. Docters T, Chovelon JM, Herrmann JM. Syntheses of TiO<sub>2</sub> photocatalysts by the molten salts method application to the photocatalytic degradation of prosulfuron. *Applied Catalysis B: Environmenta* 2004; 150: 219-26.
  10. Heinlaan M, Ivask A, Blinova I, Dubourguier HC, Kahru A. Toxicity of nanosized and bulk ZnO, CuO and TiO<sub>2</sub> to bacteria *Vibrio fischeri* and crustaceans *Daphnia magna* and *Thamnocephalus platyurus*. *Chemosphere* 2007; 71: 1308-16.
  11. Zhu Y, Eaton JW, Li C. Titanium dioxide nanoparticles preferentially induce cell death in transformed cells in a Bak/Bax-independent fashion. *PLoS One* 2012; 7: 50607.
  12. Aitken RJ, Chaudhry MQ, Boxall ABA, Hull M. Manufacture and use of nanomaterials: current status in the UK and global trends. *Occupa Med* 2006; 56: 300-6.
  13. Gao Y, Musoda Y, Seo WS, Ohta H, Koumoto K. TiO<sub>2</sub> nanoparticles prepared using an aqueous peroxotitanate solution. *Ceramics Intern* 2004; 30: 1365-8.
  14. Lettieri S, Pavone M, Fioravanti A, Santamaria Amato L, Maddalena P. Charge carrier processes and optical properties in TiO<sub>2</sub> and TiO<sub>2</sub>-based heterojunction photocatalysts: a review. *Materials (Basel, Switzerland)* 2021; 14: 1645.
  15. Boujday S, Wunsch F, Portes P, Bocquet JF, Justin CC. Solar energy mater. *Solar Cells* 2004; 83: 421.
  16. Carp O, Huisman CL, Reller A. Photoinduced reactivity of titanium dioxide. *Prog Solid Chem* 2004; 32: 33-177.
  17. Ruiz AM, Sakai G, Cornet A, Shimano K, Morante RJ, Yamazoe S. Insights into the structural and chemical modifications of Nb additive on TiO<sub>2</sub> nanoparticles. *Actuators B: Chem* 2004; 103: 312.
  18. Zhao J, Bowman L, Zhang X, et al. Titanium dioxide (TiO<sub>2</sub>) nanoparticles induce JB6 cell apoptosis through activation of the caspase-8/Bid and mitochondrial pathways. *J Toxicol Environ Health A* 2009; 72: 1141-9.
  19. Sundrarajan M, Gowri S. Green synthesis of titanium dioxide nanoparticles by *Nyctanthes arbor tristis* leaves extract. *Chalcogenide Letters* 2011; 8: 447-51.
  20. Selvakumaran RK, Franklin G. Prospective application of nanoparticles green synthesized using medicinal plant extracts as novel nanomedicines. *Nanotechnol Sci Applic* 2021; 14: 179-95.
  21. Bahmani M, Taherikalani M, Khaksarian M, Soroush S, Ashrafi B, Heydari R. Phytochemical profiles and antibacterial activities of hydroalcoholic extracts of *Origanum vulgare* and *Hypericum perforatum* and carvacrol and hypericin as a promising anti-staphylococcus aureus. *Mini-Rev Med Chem* 2019; 19: 923-32.
  22. Bahmani M, Taherikalani M, Khaksarian M, et al. The synergistic effect of hydroalcoholic extracts of *Origanum vulgare*, *Hypericum perforatum* and their active components carvacrol and hypericin against *Staphylococcus aureus*. *Future Sci OA* 2019; 5: Article number FSO371.
  23. Abbasi N, Khosravi A, Aidi A, Shafiei M. Biphasic response to luteolin in MG-63 osteoblast-like cells under high glucose-induced oxidative stress. *Iranian J Med Sci* 2016; 41: 118-25.
  24. Sankar R, Dhivya R, Subramanian Shivashangari K, Ravikumbar V. Wound healing activity of *Origanum vulgare* engineered titanium dioxide nanoparticles in Wistar Albino rats. *J Mater Sci Mater Med* 2014; 25: 1701-8.
  25. Clinical and Laboratory Standards Institute (CLSI). Methods for dilution antimicrobial susceptibility tests for bacteria that grow aerobically: Approved standard, eighth ed. (Document M7-A8). 2009; CLSI. Wayne.
  26. Nostro A, Sudano Roccaro A, Bisignano G, et al. Effects of oregano, carvacrol and thymol on *Staphylococcus aureus* and *Staphylococcus epidermidis* biofilms. *J Med Microbiol* 2007; 56: 519-23.
  27. Dadgar T, Ghaemi E, Asmar M, Mazandarani M, Bazueri M. Antibacterial activities of six medicinal plants against methicillin-resistant and sensitive *Staphylococcus aureus*. *Iranian J Med Arom Plants* 2007; 23: 73-85.
  28. García I, Ballesta S, Gilaberte Y, Rezusta A, Pascual A. Antimicrobial photodynamic activity of hypericin against methicillin-susceptible and resistant *Staphylococcus aureus* biofilms. *Future Microbiol* 2015; 10: 347-56.
  29. Kashef N, Karami S, Djavid GE. Phototoxic effect of hypericin alone and in combination with acetylcysteine on *Staphylococcus aureus* biofilms. *Photodiagnosis Photodyn Ther* 2015; 12: 186-92.
  30. Foster AH, Sheel WD, Sheel P, et al. Antimicrobial activity of titania/silver and titania/copper films prepared by CVD. *J Photochem Photobiol A* 2010; 216: 283-9.
  31. Huck-Pezzei VA, Pallua JD, Pezzei G, et al. Fourier transform infrared imaging analysis in discrimination studies of *St. John's wort* (*Hypericum perforatum*). *Anal Bioanal Chem* 2012; 404: 1771-8.
  32. Galehassadi M, Rezaei E, Najavand S, Mahkam M, Mohammadzadeh Gheshlaghi N. Isolation of carvacrol from *Origanum vulgare*, synthesis of some organosilicon derivatives, and investigating of its antioxidant, antibacterial activities. *Standard Sci Res Essays* 2014; 2: 438-50.
  33. Enyashin AN, Seifert G. Structure, stability and electronic properties of TiO<sub>2</sub> nanostructures. *Physica Status Solidi (b)* 2005; 242: 1361-70.
  34. Aitken RJ, Chaudhry MQ, Boxall ABA, Hull M. Manufacture and use of nanomaterials: current status in the UK and global trends. *Occupa Med* 2006; 56: 300-6.
  35. Hu T. Anti-bacterial study using nano silver doped high density polyethylene pipe. *Sustain Environ Res* 2012; 22: 153-8.
  36. Dutta RK, Nenavathu BP, Gangishetty MK, Reddy AV. Studies on antibacterial activity of ZnO nanoparticles by ROS induced lipid peroxidation. *Colloids Surf B Biointerfaces* 2012; 94: 143-50.
  37. Stoimenov PK, Klinger RL, Marchin GL, Klabunde KL. Metal oxide nanoparticles as bactericidal agents. *Langmuir* 2002; 18: 6679-86.
  38. Badireddy AR, Hotze EM, Chellam S, Alvarez P, Wiesner MR. Inactivation of bacteriophages via photosensitization of fullerol nanoparticles. *Environ Sci Technol* 2007; 41: 6627-32.
  39. Kikuchi Y, Sunada K, Iyoda T, Hashimoto K, Fujishima A. Photocatalytic bactericidal effect of TiO<sub>2</sub> thin films: dynamic view of the active oxygen species responsible for the effect. *J Photochem Photobiol A: Chem* 1997; 106: 51-6.
  40. Suttiponpanit K, Jiang J, Sahu M, Suvachittanont S, Charinpanitkul T, Biswas P. Role of surface area, primary particle size, and crystal phase on titanium dioxide nanoparticle dispersion properties. *Nanoscale Res Lett* 2011; 6: 27.
  41. Raut RW, Kolekar NS, Lakkakula JR, Mendhulkar VD, Kashid SB. Extracellular of silver nanoparticles using dried leaves of *Pongamia pinnata* (L) Pierre. *Nano-Micro Lett* 2010; 2: 106-13.
  42. Barzegary F, Jave A, Rezaei Zarch S. Antimicrobial activities of TiO<sub>2</sub> Nanoparticle Against *Escherichia coli* and *Staphylococcus aureus*. *J shahis sadoughi Uni Med Sci* 2010; 18: 39-46.
  43. Saadatmand MM, Yazdanshenas ME, Rezaei-Zarchi S, Yousefi-Telori B, Negahdary M. Investigation of anti-microbial properties of chitosan-TiO<sub>2</sub> Nanocomposite and its use on sterile gauze pads. *J Lab Sci* 2012; 6: 59-72.
  44. Aashis, Roy S, Parveen A, Anil R, Koppalkar MVN, Prasad A. Effect of Nano-titanium dioxide with different antibiotics against methicillin-resistant *Staphylococcus Aureus*. *J Biomat Nanobiotechnol* 2010; 1: 37-41.
  45. Shahsavari S. An overview of the most important medicinal plants used in Iranian traditional medicine for the treatment of kidney stones: a mini-review article. *Plant Biotechnol Persa* 2021; 3: 1: 10.52547/pbp.3.1.4
  46. Fattepur S, Nilugal KC, Darshan TT, et al. Toxicological and pharmacological activity of ethanolic extracts of *Catharanthus*



- roseus in experimental animals. *Int J Med Toxicol Legal Med* 2018; 21: 141-4.
47. Sengar M, Saxena S, Satsangee S, Jain R. Silver nanoparticles decorated functionalized multiwalled carbon nanotubes modified screen printed sensor for the voltammetric determination of butorphanol. *J Appl Organometallic Chem* 2021; 1: 95-108.
  48. Giorgadze TG, Khutsishvili IG, Melikishvili ZG, Bregadze VG. Silver atoms encapsulated in G4 PAMAM (polyamidoamine) dendrimers as a model for their use in nanomedicine for phototherapy. *Euro Chem Bull* 2020; 9: 22-7.
  49. Alwan S, Al-Saeed M, Abid H. Safety assessment and biochemical evaluation of biogenic silver nanoparticles (using bark extract of *C. zeylanicum*) in *Rattus norvegicus* rats: safety of biofabricated AgNPs (using *Cinnamomum zeylanicum* extract). *Baghdad J Biochem Appl Biol Sci* 2021; 2: 138-50.
  50. Simeon J, Thrush J, Bailey TA. Angiopoietin-like protein 4 is a chromatin-bound protein that enhances mammosphere formation *in vitro* and experimental triple-negative breast cancer brain and liver metastases *in vivo*. *J Carcinog* 2021; 20: 8.
  51. Bhale SP, Yadav AR, Pathare PG, et al. Synthesis, characterization and antimicrobial activity of transition metal complexes of 4-[(2-Hydroxy-4-Methoxyphenyl) Methyleneamino]-2, 4-Dihydro-3h-1, 2, 4-Triazole-3-Thione. *Europ Chem Bull* 2020; 9: 430-5.
  52. Ma D, Han T, Karimian M, Abbasi N, Ghaneialvar H, Zangeneh A. Immobilized Ag NPs on chitosan-biguanidine coated magnetic nanoparticles for synthesis of propargylamines and treatment of human lung cancer. *Int J Biolog Macromol* 2020; 165: 767-75.
  53. Wan AE, Khan MSB, Teo BSX, et al. Screening of antioxidant and antibacterial activity of methanolic extract of *Ipomoea aquatica* leaf and stem against bacteria causes skin infection. *Int J Med Toxicol Legal Med* 2020; 2: 169-78.
  54. Teo BSX, Gan RY, Abdul Aziz S, et al. *In vitro* evaluation of antioxidant and antibacterial activities of *Eucheuma cottonii* extract and its *in vivo* evaluation of the wound-healing activity in mice. *J Cosm Dermatol* 2021; 20: 993-1001.
  55. Palaksha MN, Ahmed M, Das S. Antibacterial activity of garlic extract on streptomycin-resistant *Staphylococcus aureus* and *Escherichia coli* solely and in synergism with streptomycin. *J Nat Sci Biol Med* 2010; 1: 12-5.
  56. Zharif N, Santosh F, Kiran CN, Fadli A, Ibrahim A, Nizam G. Synergistic effect of ethanolic extract of *melastoma malabataricum* leaves and antibiotics. *Int J Med Toxicol Leg Med* 2018; 21: 167.
  57. Karimi E, Abbasi S, Abbasi N. Thymol polymeric nanoparticle synthesis and its effects on the toxicity of high glucose on OEC cells: involvement of growth factors and integrin-linked kinase. *Drug Design, Development and Therapy* 2019; 13: 2513-32.
  58. Zhang Y, Mahdavi B, Mohammadhosseini M, et al. Green synthesis of NiO nanoparticles using *Calendula officinalis* extract: chemical characterization, antioxidant, cytotoxicity, and anti-esophageal carcinoma properties. *Arabian Journal of Chemistry* 2021; 14: 103105.
  59. Nurin RQ, Halim S. Potential pharmacotherapy of *olea europaea* (Olive) fruit oil against methamphetamine-induced neurotoxicity. *Journal of Cellular and Molecular Anesthesia* 2019; 4: 67-8.
  60. Khalep HRH, Abidin AZ, Hassan H, Fattapur S, Othman Z. The anti-angiogenic properties of *Morinda Citrifolia L.* (Mengkudu) leaves using chicken chorioallantoic membrane (CAM) assay. *Pharmacognosy Journal* 2019; 11: 12-5.
  61. Sathi SS, Kiran CN, Santosh F, Fadli A, May F, Ibrahim A, Jiyauddin K. Comparison of wound healing activity of piper betle and *ocimum sanctum* in wistar rats. *International Journal of Medical Toxicology and Legal Medicine* 2020; 23: 109-16.
  62. Kaleemullah M, Jiyauddin K, Thiban E, Rasha S, Al-Dhalli S, Budiasih ., Gamal OE, Fadli A, Eddy Y. Development and evaluation of Ketoprofen sustained release matrix tablet using *Hibiscus rosa-sinensis* leaves mucilage. *Saudi Pharmaceutical J* 2017; 25: 770-9.